

The Pennsylvania State University

The Graduate School

Department of Chemistry

POLYOL SYNTHESIS OF PALLADIUM HYDRIDE:

BULK POWDERS VS. NANOCRYSTALS

A Thesis in

Chemistry

by

Ting-Hao Phan

© 2009 Ting-Hao Phan

Submitted in Partial Fulfillment
of the Requirements
for the Degree of

Master of Science

August 2009

The thesis of Ting-Hao Phan was reviewed and approved* by the following:

Raymond E. Schaak
Associate Professor of Chemistry
Thesis Advisor

Alan J. Benesi
Professor of Chemistry
Director of the NMR Facility and Lecturer in Chemistry

Christine D. Keating
Associate Professor of Chemistry

Barbara J. Garrison
Head of the Chemistry Department
Shapiro Professor of Chemistry

*Signatures are on file in the Graduate School

ABSTRACT

Hydrogen is an environmentally friendly energy carrier with light weight, high energy density, and high abundance. However, the lack of suitable hydrogen storage material limits the feasibility of the technology. Recently, metal and intermetallic hydrides are considered as potential hydrogen storage materials. Therefore, development of a facile chemical method for synthesizing hydrogen storage materials is very important in this field of work. In this study, we described a polyol-based chemical route for converting Pd powders and nanocrystals into β -PdH_x using NaBH₄ as hydrogen source. Different behaviors of hydrogen absorption, storage, and release between bulk and nanocrystalline palladium were also studied.

Nanocrystalline Pd absorbs hydrogen at lower temperatures than bulk Pd. Bulk palladium reacted with NaBH₄ in tetraethylene glycol to form β -PdH_x completely at 190 °C, while complete conversion to β -PdH_x occurred at 120 °C for palladium nanocrystals. Also, nanocrystalline palladium reacts to form PdH_x much faster at 90 °C, as well as has faster kinetics of desorbing hydrogen than bulk palladium.

Well-dispersed palladium nanocrystals of about 6 to 16 nm were synthesized with ethylene glycol as reducing agent and PVP as capping agent. The general size and morphology of the Pd nanocrystals are retained after absorbing hydrogen to form β -PdH_x, as well as after releasing hydrogen to re-form Pd.

Palladium powders could not convert into PdH_x with bubbling H₂ under otherwise identical reaction conditions. This indicates that palladium would not convert into PdH_x via simply absorbing H₂ gas decomposed from NaBH₄, but through dissociating BH₄⁻ and then absorbing chemisorbed H atoms into its lattice.

TABLE OF CONTENTS

LIST OF FIGURES.....	v
ACKNOWLEDGEMENTS.....	vi
Chapter 1 Converting palladium powders and nanocrystals into palladium hydride....	1
1.1 Introduction.....	1
1.2 Experimental.....	6
1.2.1 Materials.....	6
1.2.2 Synthesis methods.....	7
1.2.2.1 Synthesis of bulk palladium hydride.....	7
1.2.2.2 Synthesis of nanocrystalline palladium hydride.....	7
1.2.3 Characterization.....	8
1.3 Results and discussion.....	9
1.3.1 Temperature study for converting Pd to β -PdH _x	9
1.3.2 Kinetic study of hydrogen absorption and desorption on Pd.....	12
1.3.3 Morphology study for hydriding and dehydriding reactions.....	16
1.3.4 Mechanism of borohydride-assisted hydriding process.....	20
1.4 Conclusions.....	22
References.....	24
Appendix Resume.....	28

LIST OF FIGURES

<p>Figure 1-1: Powder XRD patterns for (a) bulk Pd and (b) nanocrystalline Pd reacted with NaBH₄ in TEG at the temperatures indicated. Complete conversion to PdH_x occurs at 190 °C for bulk Pd and 120 °C for nano-Pd. Vertical dashed lines indicate the peak positions for Pd.....</p>	10
<p>Figure 1-2: GC profile showing hydrogen released after heating bulk PdH_x in a closed system, confirming the presence of hydrogen in the Pd lattice. A slight nitrogen impurity is present from the collection atmosphere.....</p>	11
<p>Figure 1-3: Powder XRD patterns showing the time-dependent reactivity of (a) bulk Pd and (b) nano-Pd. In (a), bulk Pd (i) was reacted with NaBH₄ in TEG for (ii) 10 min and (iii) 60 min, and then fresh NaBH₄ was added and reacted for an additional (iv) 10 min and (v) 60 min. In (b), nanocrystalline Pd (i) was reacted with NaBH₄ in TEG for (ii) 1 min, (iii) 5 min, and (iv) 10 min, then (v) an additional 10 min after adding fresh NaBH₄. Vertical dashed lines indicate the positions of the <i>111</i> and <i>200</i> peaks for Pd.....</p>	12
<p>Figure 1-4: Powder XRD patterns showing hydrogen release for bulk and nanocrystalline PdH_x. For bulk PdH_x (bottom), heating to 180 °C releases some of the hydrogen, generating PdH_x with a smaller hydrogen content along with some Pd. For nano-Pd (top), heating to 180 °C releases all of the hydrogen, generating only nano-Pd as a product. Vertical dashed lines indicate the peak positions for Pd.....</p>	14
<p>Figure 1-5: TEM images and corresponding SAED patterns of (a) Pd nanocrystals and (b) β-PdH_x nanocrystals.....</p>	17
<p>Figure 1-6: TEM images and corresponding particle size distribution of (a) Pd nanocrystals, (b) PdH_x nanocrystals after reaction with NaBH₄ in TEG, and (c) re-generated Pd nanocrystals after hydrogen release. Scale bars in (a), (b), and (c) correspond to 20 nm. Percentages are based on 200 particles for each sample.....</p>	18
<p>Figure 1-7: TGA data of polyol-synthesized Pd nanocrystal.....</p>	19
<p>Figure 1-8: Powder XRD patterns for (a) bulk Pd reacted with bubbling H₂ in TEG at 190 °C, (b) bulk Pd reacted with NaBH₄ in H₂O in an autoclave at 190 °C, (c) bulk Pd reacted with NaBH₄ in TEG in an autoclave at 190 °C. Vertical dashed lines indicate the peak positions for Pd.....</p>	21
<p>Figure 1-9: Mechanism of Pd-catalyzed borohydride hydrolysis in H₂O [31].....</p>	22

ACKNOWLEDGEMENTS

I would like to thank Dr. Raymond Schaak, my advisor, for giving me the opportunity to work with him at Texas A&M University and the Pennsylvania State University. I also appreciate Dr. Schaak for his insightful advice, consistent guidance and encouragement on every aspect of my research and my life. I would like to thank my committee members, Dr. Christine Keating and Dr. Alan Benesi, for their helpful comments regarding my research.

I would like to acknowledge all my colleagues for creating a cordial working atmosphere. To name but a few: Dr. Brian Leonard helped me a lot on the synthesis of intermetallic compounds and orthogonal reactivity of metals. Dr. Beth Anderson and Dr. Karl Oyler who helped me in my seminar presentation and their helpful discussions regarding research experiments was greatly appreciated. Zachary Schaefer, who helped me in my academic research and introduced me to American culture. Finally, I want to thank James Bondi who always created a friendly environment and made me feel relaxed in the lab all the time.

Moreover, I would like to acknowledge my parents, brother, and girlfriend for encouraging me to study Chemistry in the United States. They have always offered me a safe harbor and are willing to open their arms to me when I am troubled. I could do nothing without their support.

At last, this research was mainly supported by the US Department of Energy under grant NO. DE-FG02-08ER46483 and the Petroleum Research Fund. This thesis is also reproduced by permission of The Royal Society of Chemistry (<http://www.rsc.org/Publishing/Journals/CC/article.asp?doi=b902024a>).

CHAPTER 1

CONVERTING PALLADIUM POWDERS AND NANOCRYSTALS INTO PALLADIUM HYDRIDE

1.1 Introduction

Natural resources on the planet Earth are limited, but the energy we consume increases significantly every year. While the national economy strongly relies on the limited fossil fuel supplies, as well as severe environmental issues associated with petroleum, new kinds of energy sources should be developed instantly. Hydrogen-based fuel system is one of the more desirable energy sources for the replacement of fossil fuels. Hydrogen is an environmentally friendly energy carrier with light weight, high energy density, and high abundance. However, there are safety problems associated with using compressed gas tanks as hydrogen storage materials, because of high pressure of the tank. A heavy stainless steel gas tank is also required, reducing the convenience of hydrogen fuel cells.

According to Hydrogen-storage requirements targeted by the United States Department of Energy, a viable hydrogen storage system should provide the gravimetric capacity of 4.5 wt% in 2010, and 5.5 wt% in 2015. In order to achieve the DOE hydrogen-storage targets, metal and intermetallic hydrides are considered as potential hydrogen storage media due to their gravimetric and volumetric storage capacities and safe working conditions above room temperature, improving practical usage of hydrogen fuel cells. Among metal and intermetallic hydrides, palladium hydride, PdH_x, is one of the most well-studied prototype materials for hydrogen-based fuel systems. The properties of readily absorbing and dissociating

hydrogen into its lattice, as well as the noble character of palladium make palladium hydride attract extensive research activities, though the gravimetric capacity of palladium hydride is not great enough for practical usage.

Besides hydrogen storage media, Pd has been investigated as a hydrogen dissociation catalyst for activation of other hydrogen storage materials. Shan et al. [2] reported that mechanical grinding of alloys, $\text{LaNi}_{4.7}\text{Al}_{0.3}$, CaNi_5 or Mg_2Ni , with 1 to 10 wt% Pd reduced the activation pressure for hydriding samples from more than 1 MPa to 100 KPa H_2 at room temperature. In addition, this small amount of Pd not only increased the hydrogen absorption and desorption rate, but also significantly improved the stability of intermetallic alloys under air atmosphere [3]. They suggested that the hydrogen storage performances of air-sensitive intermetallic alloys were improved via hydrogen spillover and reverse hydrogen spillover through Pd particles adhering to the surface of the alloys. Sabo et al. [4] reported that doping 1 wt % Pd into porous metal-organic framework MOF-5 enhanced hydrogen storage capacity. They mixed a solution of $\text{Pd}(\text{acac})_2$ and guest-free MOF-5, followed by reducing Pd^{2+} ions at 100 °C under H_2 atmosphere for 1h. They claimed that a hydrogen spillover effect through doping MOF-5 with Pd improved hydrogen storage capacity of MOF-5 from 1.15 wt% to 1.86 wt% at 1 atm and 77 K. Based on the spillover effect of Pd, Jung's group [5] reported that the hydrogen storage capacity of double-walled silica nanotubes was increased by loading with Pd nanoparticles. The hydrogen storage capacity of the raw material was only 0.1 wt% at 298 K. After loading 10 wt% Pd, the hydrogen storage capacity dramatically increased to 1.9 wt %. Even over several repeated adsorption and desorption cycles, a constant hydrogen storage capacity was accomplished, improving practical usage of double-walled silica nanotubes for hydrogen storage.

In addition to hydrogen dissociation catalyst, Pd can function as a

hydrogen-permeable membrane for transport, separation, and purification. It is known that H₂ can be produced by steam reforming of hydrocarbons. However, an additional process of hydrogen purification is necessary due to the formation of by-products, such as CO₂ and CO. Lin et al. [6] developed a multi-tube Pd membrane separator to produce high purity hydrogen from catalytic reformer stream gas. The Pd membranes prepared by electroless plating on porous stainless steel performed with a high selectivity of H₂/N₂ in range of 200 – 1400, as well as permeance of hydrogen in range of 3 – 7 m³/m²-h-atm.

Pd has also been significantly investigated for its applications in sensing. Im et al. [7] fabricated single Pd nanowire between gold electrodes as a hydrogen sensor with ultralow power consumption. The shape of the single Pd nanowire sensor can be well controlled by electrodeposition from 100 nm to 1 μm in diameter and up to 7 μm in length. They found the Pd nanowire resistance was reduced while hydrogen gas was present, resulting in enhancement of output voltage. Output voltage was further enhanced as the concentration of hydrogen was increased (between 0.02 and 10 % in N₂ gas). Also, the response of Pd nanowire sensor to hydrogen was rapid and reversible.

PdH_x is also interesting for its composition-dependent superconducting properties. In 1972 Skoskiewicz et al. [8] observed superconductivity in palladium hydride when the atomic ratio of hydrogen to palladium was above 0.83. They demonstrated that the critical temperature, the highest temperature for a material holding its superconducting properties, was raised with increasing the content of hydrogen in Pd. The highest critical temperature of 9.1 K was found by Strizker's group [9].

PdH_x most commonly exists in two forms, α-PdH_x (fcc, 0 < x < 0.02) and β-PdH_x (fcc, 0.58 < x < 1). Maeland's group [10] reported that the lattice constant

of pure Pd is $a = 3.889 \text{ \AA}$. In the α phase of palladium hydride, Pd dissolves a small amount of hydrogen in its lattice and undergoes an isotropic expansion with the lattice constant of $a = 3.895 \text{ \AA}$ [11]. The isotropic expansion of the lattice is attributed to inserting hydrogen atoms, occupying octahedral interstices in the fcc Pd lattice, as well as increasing separation of nearest-neighbor metals. As hydrogen is further absorbed, a more stable phase, β -PdH_x, nucleates through a phase transition and the lattice expands abruptly to $a = 4.025 \text{ \AA}$. Schirber et al. [12] observed that the lattice constant of β -PdH_x is composition-dependent, varying from about 4.02 \AA to 4.08 \AA as the content of hydrogen in Pd increases.

Palladium hydrides are typically formed by gas-phase hydrogen absorption and high-pressure hydrogen insertion. In 1944, Owen et al. [13] charged Pd with gas-phase hydrogen and measured the lattice constant under various temperatures and hydrogen pressures. They observed that α -PdH_x started converting to β -PdH_x under 100 torr of H₂ at 60 °C and demonstrated that the H₂ pressure for converting Pd to PdH_x is increased as the reaction temperature is elevated. Antonov's group [14] increased hydrogen pressure to enhance the solubility of hydrogen in Pd. They found that the H/Pd stoichiometric ratio can reach about 1 under a pressure of 90 kbar above 200 °C.

Electrochemical reaction with palladium is another method to fabricate PdH_x. Bernardini et al. [15] investigated electrolytic hydrogen loading into Pd electrodes using 85% and 100% H₃PO₄ as electrolytes. They observed that the H/Pd stoichiometric ratio of 0.8 can be achieved under -0.5 V, which is as efficient as about 50 atm hydrogen gas while applying high-pressure hydrogen insertion. However, the efficiency of electrolytic loading decreased with increasing temperature due to the formation of phosphine, PH₃, which is a weak hydrogen promoter.

An alternative and mild solution chemistry method, introduced by Murphy et al. [16], is to react bulk Pd, as well as bulk-scale hydrogen-absorbing intermetallic compounds, with aqueous borohydride to form metal and intermetallic hydrides. They claimed that metal and intermetallic hydrides were produced via reacting 50 ml of 2.6 M aqueous solution of NaBH₄ with 1 g of starting materials at room temperature, followed by stirring overnight in a beaker. This study very effectively demonstrated the versatility and materials generality of low-temperature ambient-pressure chemical methods for hydrogen insertion into metals and intermetallics.

While Murphy's work focused on bulk-scale materials, applying the borohydride method to nanocrystalline metals and intermetallic compounds is highly intriguing. Nanocrystalline hydrides have been widely investigated because their properties are usually size dependent and different to bulk properties. Balde et al. [17] observed that decreasing the particle sizes of sodium alanate to nano-scale dimensions significantly lowered hydrogen desorption temperatures, hydrogen reloading pressures, and activation energies. Horinouchi's group [18] demonstrated that palladium nanoparticles have faster hydriding and dehydriding reaction rates than bulk palladium. They also mentioned that reducing the particle size of Pd increases the maximum α -phase hydrogen concentration, as well as decreases the minimum β -phase hydrogen concentration, resulting in a narrower two-phase plateau region in the hydrogen pressure-composition isotherm. Yamauchi et al. [19] claimed that the faster kinetics of absorption and desorption and size-dependent hydrogen contents were attributed to weaker chemical bonds between hydrogen and palladium atoms in the nanometer sized particles. Also, non-equilibrium phases can be stabilized in nanocrystalline solids prepared through low-temperature solution routes. For example, Vasquez et al. [20] synthesized non-equilibrium intermetallic nanocrystals, Au₃Fe,

Au₃Ni and Au₃Co, with the L1₂ (Cu₃Au) structure at 250 °C using octyl ether as a solvent. Dawood et al. [21] fabricated wurtzite-type ZnS and ZnSe nanocrystals using wurtzite-type ZnO as a structural template in the presence of ethylene glycol. Similar approaches for hydrides could lead to the discovery of new hydrogen storage materials and perhaps hydride materials with enhanced absorption capabilities.

In this work, we describe a facile polyol-based chemical route for converting Pd powders and nanocrystals into PdH_x. The polyol process is one of the more desirable chemical methods for nanocrystal synthesis. Ducamp-Sanguesa's group [22] produced palladium black powder with an average particle size of 100 Å using ethylene glycol as solvent and reducing agent. Xia and his coworkers [23] synthesized various morphologies of Pd nanocrystals, such as plates, octahedra and cubes, in ethylene glycol using polyvinyl pyrrolidone (PVP) and bromide ions as capping agents. This study effectively merges the polyol process with metal hydrides and describes a facile polyol-based chemical route for converting Pd powders and nanocrystals into PdH_x using NaBH₄ as hydrogen source, experimentally demonstrating the different behaviors of hydrogen absorption, storage, and release between bulk and nanocrystalline palladium.

1.2 Experimental

1.2.1 Materials

Bulk palladium powder (0.25-0.55 μm, 99.95%), sodium borohydride (NaBH₄, 98%), and tetraethylene glycol (TEG, 99%) were purchased from Alfa Aesar. Palladium salt, Na₂PdCl₄, was purchased from Acros Organic. Ethylene glycol (EG,

99%) was purchased from JT Baker. Poly(vinyl pyrrolidone) (PVP, MW = 55,000) was purchased from Sigma Aldrich. All chemicals obtained from commercial sources were used as received without additional purification.

1.2.2 Synthesis methods

1.2.2.1 Synthesis of bulk palladium hydride

20 mg of bulk palladium powder was dispersed in 20 mL of TEG in a 100 mL three-neck round flask via sonication, followed by heating to 90 – 210 °C while stirring with magnetic bar and bubbling with Ar. A fresh solution of 3 mL of TEG and 45 mg of NaBH₄ was added dropwise to the hot TEG solution containing Pd powder while stirring for 2 min. The resulting solution was then slowly cooled down to room temperature. The particles were collected through centrifugation, washed with ethanol, and then dried at room temperature.

1.2.2.2 Synthesis of nanocrystalline palladium hydride

Polyol-synthesized Pd nanocrystals have good stability, offering narrow particle size distribution for the following conversion process. The procedure of synthesizing Pd nanocrystals is modified from Xia's study [24]. Pd nanocrystals were synthesized by heating 7 mL of EG in a 50 ml three-neck round flask to 110 °C while stirring with magnetic bar and holding the temperature for 1 h under an air purge, followed by simultaneously injecting a 3.3 mL EG solution of Na₂PdCl₄ (135 mg) and a 3.3 mL

EG solution of PVP (80 mg) into round flask at a rate of 45 mL per hour at 110 °C. The resulting solution was then stirred for 3 h at 110 °C under an air purge. Pd²⁺ ions were reduced to Pd nanocrystals by hot EG in the presence of PVP. The resulting Pd nanocrystals were isolated with acetone through centrifugation, washed with ethanol, and then dried under vacuum at room temperature.

25 mg of nanocrystalline Pd was re-dispersed in 10 mL of TEG with 20 mg of PVP via sonication. This Pd dispersion was added into 20 mL of heated TEG along with additional 10 mg of PVP at 90 – 190 °C in a 100 ml three-neck round flask under purging Ar gas, followed by dropwise addition of a solution of 45 mg of NaBH₄ in 3 mL of TEG with stirring for 2 min. The resulting nanocrystalline palladium hydride was isolated, washed with ethanol through centrifugation, and dried at room temperature.

1.2.3 Characterization

Powder X-ray diffraction patterns were collected on a Bruker Advance D8 X-ray diffractometer with Cu K α radiation ($\lambda = 1.5418 \text{ \AA}$). Powder X-ray diffraction (XRD) is a useful tool in this study for characterizing the formation of PdH_x by hydrogen insertion into Pd, because of the composition-dependent lattice expansion [12].

Transmission electron microscopy (TEM) and selected area electron diffraction (SAED) data were recorded using a JEOL JEM 1200EX-II operating at 80 kV. Samples for TEM analysis were prepared by dispersing nanocrystals in ethanol and depositing a drop of dispersion onto a carbon coated nickel grid, followed by evaporating the solvent.

Gas chromatography (GC) measurements were performed on a Varian Aerograph Model 90-P with a thermal conductivity detector (TCD) and room temperature molecular sieve column. Samples for GC analysis were prepared in an Ar-purged glove box. A vial containing 20 mg of sample was then set in a sand bath, followed by heating to 250 °C for 1h. After heating, a gas sample from the headspace was measured by GC with a thermal conductivity detector.

Thermogravimetric analysis (TGA) was collected on a TA Instruments SDT Q600. 5-10 mg of sample was placed in alumina crucibles. After the reaction chamber was purged by flowing Ar for 30 min the sample was measured by TGA with a heating rate of 10 °C min⁻¹ under a 100 mL min⁻¹ flow of Ar.

1.3 Results and discussions

1.3.1 Temperature study for converting Pd to β -PdH_x

In order to investigate the effect of particle size on hydrogen insertion into Pd, various reaction temperatures were used in converting Pd to β -PdH_x. Figure 1-1 shows powder X-ray diffraction (XRD) data for bulk (0.25-0.55 μ m) and nanocrystalline (6-16 nm) Pd reacted with NaBH₄ in TEG for 2 min at different temperatures.

It is known that pure Pd has a lattice constant of $a = 3.889 \text{ \AA}$, α -PdH_x has $a \approx 3.895 \text{ \AA}$, and β -PdH_x has $a \approx 4.025 \text{ \AA}$. Schirber et al. [12] observed the lattice constant of β -PdH_x varies from about 4.02 \AA to 4.08 \AA as the content of hydrogen in Pd increases. The bulk and nanocrystalline Pd samples were both found to have lattice constants of $a = 3.89 \text{ \AA}$, which matches the literature values. As the reaction

temperature increases, the XRD pattern for bulk Pd changes to a multi-phase fcc sample that is consistent with lattice expansion due to hydrogen insertion into the Pd lattice.

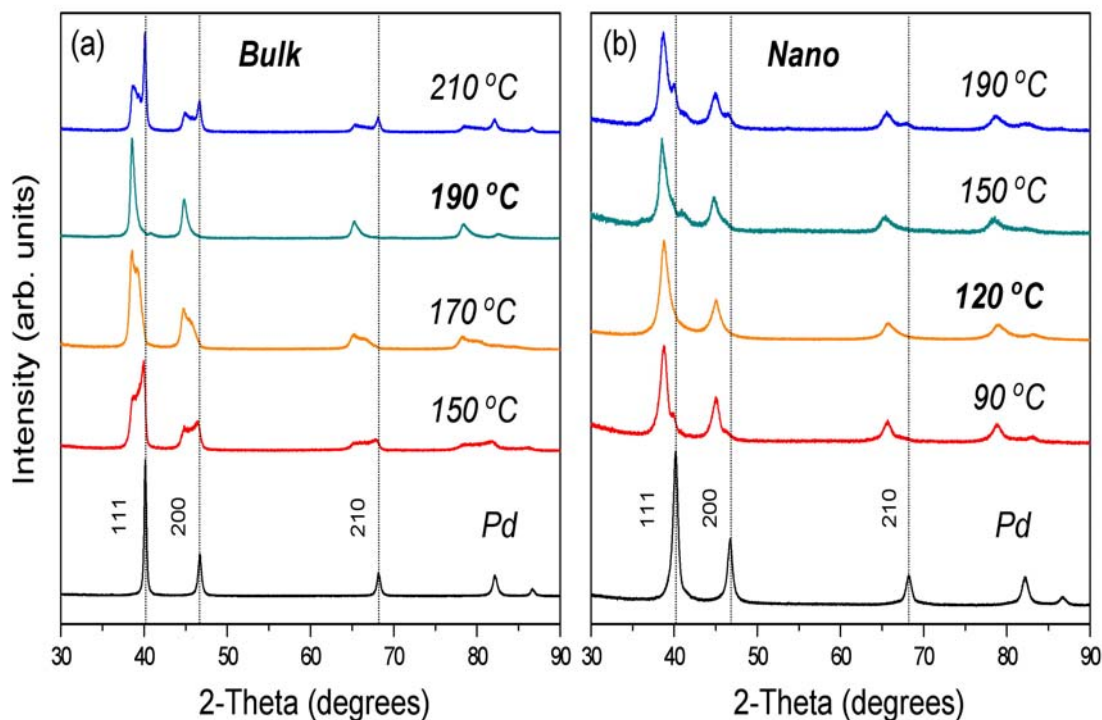


Fig 1-1 Powder XRD patterns for (a) bulk Pd and (b) nanocrystalline Pd reacted with NaBH₄ in TEG at the temperatures indicated. Complete conversion to PdH_x occurs at 190 °C for bulk Pd and 120 °C for nano-Pd. Vertical dashed lines indicate the peak positions for Pd.

Gas chromatography (GC) data, shown in Figure 1-2, confirmed the presence of hydrogen in the PdH_x products, based on pure H₂ as the standard for determining retention times. After heating bulk PdH_x in a closed system, hydrogen gas was detected in the headspace, while heating bulk Pd under identical closed-system conditions showed no hydrogen. A small nitrogen impurity is also present from the collection atmosphere. This GC data clearly confirms that the lattice expansion observed by XRD is attributable to hydrogen absorption.

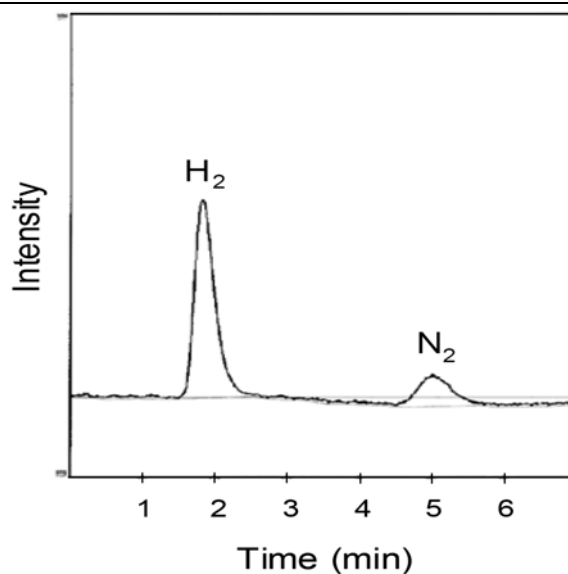


Fig 1-2 GC profile showing hydrogen released after heating bulk PdH_x in a closed system, confirming the presence of hydrogen in the Pd lattice. A slight nitrogen impurity is present from the collection atmosphere.

At 190 °C, for bulk Pd a nearly phase-pure fcc pattern with $a = 4.040 \text{ \AA}$ is evident. This corresponds to β -PdH_x with $x \approx 0.7$, based on comparison with Schirber's report. Heating to higher temperatures in solution returns the sample to predominantly Pd. Nanocrystalline Pd shows a similar trend, reacting with borohydride under identical conditions to form β -PdH_x ($a = 4.037 \text{ \AA}$), followed by gradually returning to a multi-phase fcc sample as the temperature increases. However, most of the nanocrystalline Pd is converted to PdH_x as low as 90 °C, with phase-pure PdH_x observed at 120 °C. Moreover, β -PdH_x is the dominant phase for nanocrystalline Pd in the temperature range from 90 °C to 190 °C. Thus, nanocrystalline Pd reacts with NaBH₄ in polyol solution not only forming a hydride at a significantly lower temperature, but also over a wider range of reaction temperatures than bulk Pd under otherwise identical reaction conditions.

1.3.2 Kinetic study of hydrogen absorption and desorption on Pd

In order to investigate the effect of particle size on the efficiency of hydrogen absorption and desorption, we reacted bulk and nanocrystalline Pd with NaBH₄ in TEG at 90 °C, and then heated samples to 180 °C for 4 h in a tube furnace under Ar. Figure 1-3 shows powder XRD data for the results of bulk and nanocrystalline Pd with NaBH₄ in TEG at 90 °C.

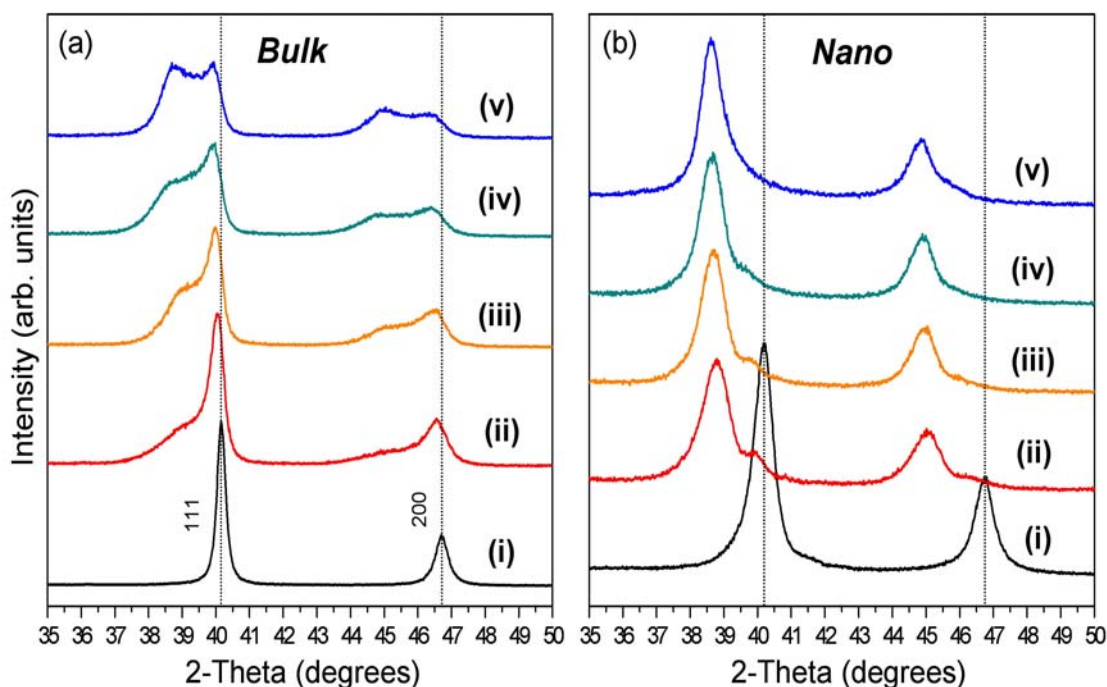


Fig 1-3 Powder XRD patterns showing the time-dependent reactivity of (a) bulk Pd and (b) nano-Pd. In (a), bulk Pd (i) was reacted with NaBH₄ in TEG for (ii) 10 min and (iii) 60 min, and then fresh NaBH₄ was added and reacted for an additional (iv) 10 min and (v) 60 min. In (b), nanocrystalline Pd (i) was reacted with NaBH₄ in TEG for (ii) 1 min, (iii) 5 min, and (iv) 10 min, then (v) an additional 10 min after adding fresh NaBH₄. Vertical dashed lines indicate the positions of the *111* and *200* peaks for Pd.

After 10 min, most of bulk Pd has converted to α -PdH_x with lattice constants

of $a = 3.899 \text{ \AA}$, as evidenced by the slight shift of XRD peaks to low angles is also observed. The emergence of shoulders to the left of the 111 and 200 peaks of Pd indicates the growth of $\beta\text{-PdH}_x$. Based on quantitative analysis of the phase fractions, only 43% of bulk Pd has converted to $\beta\text{-PdH}_x$. After 60 min, slightly more of the sample has been converted to $\beta\text{-PdH}_x$ (54%). However, the reaction is not yet complete, possibly from decomposition and subsequent lack of availability of the NaBH_4 during the long reaction time. When the solution is replenished with a fresh solution of NaBH_4 , the phase fraction of $\beta\text{-PdH}_x$ again begins to increase. After reaction for an additional 60 min, a maximum of 74% of bulk Pd has converted to $\beta\text{-PdH}_x$. However, conversion to PdH_x is not complete at $90 \text{ }^\circ\text{C}$. In contrast, 91% of the nanocrystalline Pd has converted to $\beta\text{-PdH}_x$ after only 1 min of reaction with NaBH_4 in TEG at $90 \text{ }^\circ\text{C}$, with almost phase-pure $\beta\text{-PdH}_x$ formed within 10 min. The second injection of a fresh solution of NaBH_4 does not significantly affect the XRD pattern of nanocrystalline $\beta\text{-PdH}_x$, indicating that the maximum of hydrogen absorption for Pd nanocrystals is accomplished after the first addition of NaBH_4 . Thus, nanocrystalline PdH_x forms much faster than its bulk analogue.

In addition to faster conversion of Pd to PdH_x at lower temperatures for nanocrystalline vs. bulk Pd, nanocrystalline PdH_x can release the hydrogen to re-form Pd faster than bulk Pd. Figure 1-4 shows powder XRD data for the purest attainable samples of bulk and nanocrystalline PdH_x , as well as these samples heated to $180 \text{ }^\circ\text{C}$ for 4 h in a tube furnace under Ar.

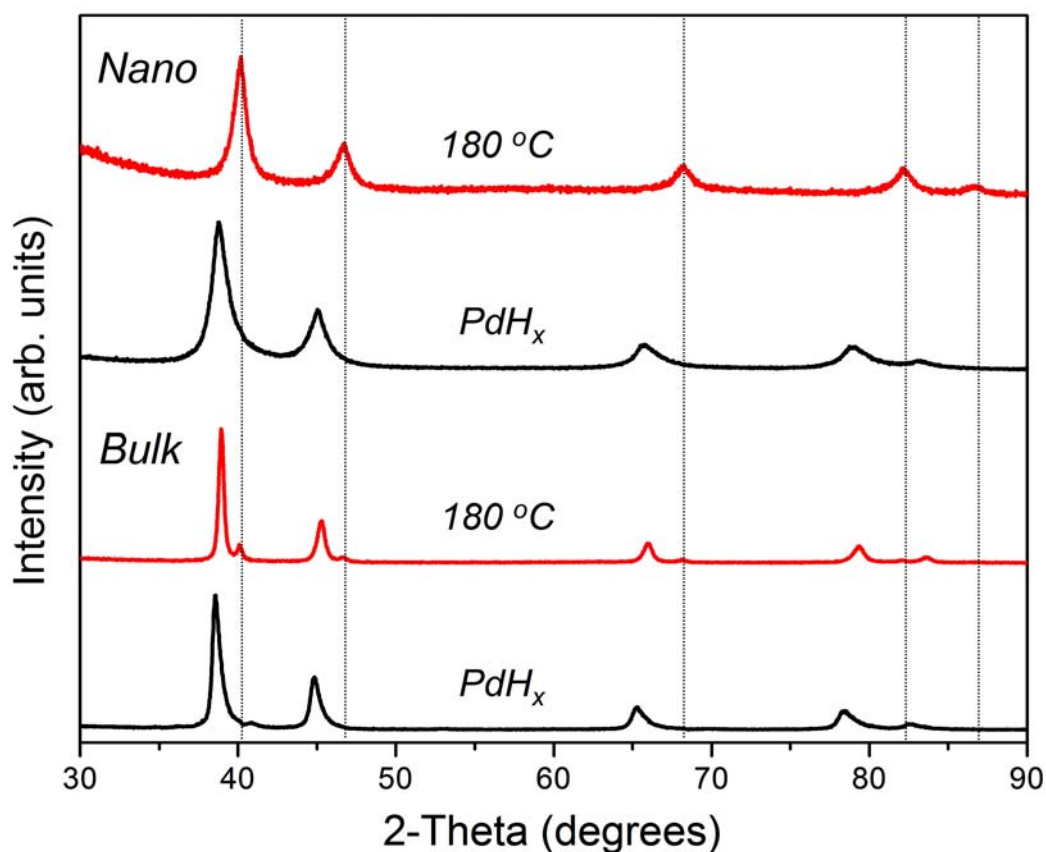


Fig 1-4 Powder XRD patterns showing hydrogen release for bulk and nanocrystalline PdH_x. For bulk PdH_x (bottom), heating to 180 °C releases some of the hydrogen, generating PdH_x with a smaller hydrogen content along with some Pd. For nano-Pd (top), heating to 180 °C releases all of the hydrogen, generating only nano-Pd as a product. Vertical dashed lines indicate the peak positions for Pd.

Under these conditions, bulk β -PdH_x has begun to release hydrogen to form a hydride phase with lower hydrogen content ($a = 4.00 \text{ \AA}$ after heating vs. $a = 4.04 \text{ \AA}$ before heating), as well as a small amount of Pd. In contrast, nanocrystalline β -PdH_x has released almost all of the hydrogen under these conditions, as indicated by the XRD pattern showing nearly phase-pure Pd without any evidence of β -PdH_x. Thus, nanocrystalline Pd can absorb and desorb hydrogen atoms significantly faster than bulk Pd.

Amorim et al. [25] reported that the decomposition temperature of bulk β -PdH_x

prepared by gas-phase hydrogen absorption is 113 °C. However, β -PdH_x in our work releases hydrogen starting around at 180 °C. Differences in desorption behavior between β -PdH_x prepared using traditional methods and those made in polyol solution could arise from some solvent decomposition and subsequent carbon inclusion, either coating the surface or intercalated into the structure, or interstitial boron from the borohydride. These impurities would retard the diffusion rate of hydrogen in Pd lattice, as well as increase the stability of bulk β -PdH_x.

It is worth pointing out that, compared to bulk systems, nanocrystalline Pd has faster kinetics of absorbing and desorbing hydrogen than bulk analogues, which can be attributed to nanoscale size effects. Nanocrystalline Pd has more reaction sites due to its high surface-to-volume ratio, resulting in faster hydrogen absorption when reacting with borohydride. Moreover, hydrogen atoms move faster in Pd nanocrystals than in bulk Pd. Yamauchi et al. [19] reported both the heat of formation ($\Delta H_{\alpha \rightarrow \beta}$) and the entropy change ($\Delta S_{\alpha \rightarrow \beta}$) associated with hydride formation in nanocrystals are reduced. This indicates that the subsurface is deformed to generate a relatively loose lattice structure in nanocrystalline Pd, producing a weaker chemical bond between hydrogen and palladium atoms, as well as offering hydrogen a larger degree of freedom. Also, the fraction of the subsurface in Pd nanocrystals is higher than in Pd bulk, allowing hydrogen atoms to diffuse through Pd nanoparticles rapidly. Furthermore, reducing the diffusion pathway facilitates hydriding and dehydriding. Millet et al. [26] found that the hydrogen diffusion rate in the α phase is smaller than in the β phase through applying an electrochemical method. The calculated diffusion coefficients of hydrogen in palladium are $1 \times 10^{-7} \text{ cm}^2 \text{ S}^{-1}$ in the α phase and $5.5 \times 10^{-7} \text{ cm}^2 \text{ S}^{-1}$ in the β phase. This implies that the permeation of hydrogen through the α -phase layer may become the rate-determining step during the formation of hydrides. Therefore, nanocrystalline Pd minimizes the transport path of hydrogen through the α

phase region, significantly facilitating hydriding and dehydriding the entire Pd particles.

Another thing worth demonstrating is hydrogen storage capacity. It is known that reducing the particle size of Pd decreases the minimum β -phase hydrogen concentration, because it is difficult for the deformed α -phase subsurface layer in nanocrystalline Pd to convert ordered β -phase hydride [27]. Therefore, it is necessary to control particle size to discover an optimal balance between hydrogen storage capacity and kinetics. According to XRD data of our samples, the lattice constant of bulk β -PdH_x is slightly larger than that of nanocrystalline β -PdH_x ($a = 4.04 \text{ \AA}$ for bulk β -PdH_x vs. $a = 4.037 \text{ \AA}$ for nanocrystalline β -PdH_x). We could roughly estimate that the hydrogen storage capacities of bulk and nanocrystalline Pd are close to a H/Pd stoichiometric ratio of 0.7, implying that the number of absorption sites is similar between bulk and nanocrystalline Pd in this study. Thus, we reported a facile polyol-based chemical method for synthesizing nanocrystalline β -PdH_x with faster kinetics of absorbing and desorbing hydrogen, as well as high hydrogen storage capacities.

1.3.3 Morphology study for hydriding and dehydriding reactions

Figure **1-5a** shows a TEM image and selected area electron diffraction (SAED) pattern for the Pd nanocrystals that were synthesized as described earlier. These nanocrystals were then isolated, washed several times, and re-dispersed in fresh TEG before adding NaBH₄ and heating to 120 °C to form PdH_x. The TEM image in Figure **1-5b** shows that the resulting PdH_x nanocrystals are of similar size and shape to the Pd nanocrystal precursors. Quantitative analysis of the SAED patterns

for PdH_x confirms that the nanocrystals correspond to the hydride: $a = 3.9 \text{ \AA}$ for the Pd nanocrystals in Figure 1-5a and $a = 4.1 \text{ \AA}$ for the PdH_x nanocrystals in Figure 1-5b.

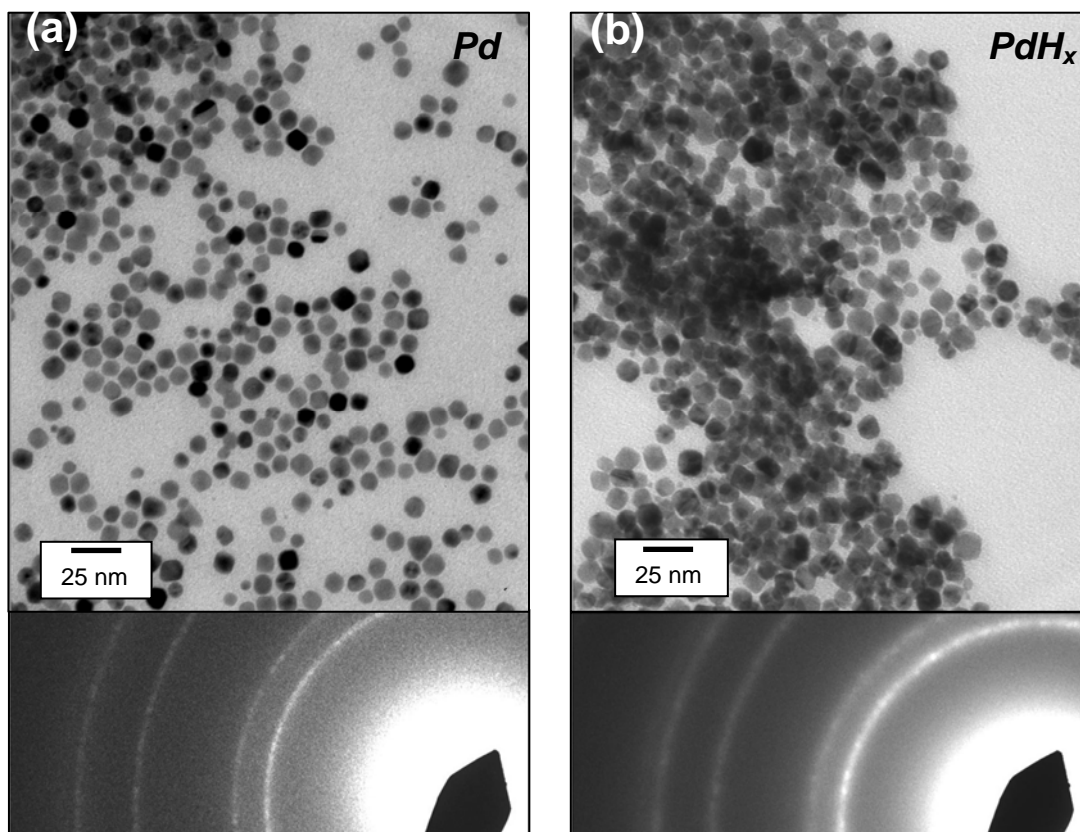


Fig 1-5 TEM images and corresponding SAED patterns of (a) Pd nanocrystals and (b) β-PdH_x nanocrystals.

The general size and morphology of the Pd nanocrystals are retained after absorbing hydrogen to form β-PdH_x, as well as after releasing hydrogen to re-form Pd. Figure 1-6a shows that a TEM image of a sample of Pd nanocrystals with an average particle size of $10.4 \pm 1.9 \text{ nm}$ and Figure 1-6b shows this same sample with an average particle size of $10.8 \pm 2.3 \text{ nm}$ after conversion to β-PdH_x. Figure 1-6c shows the nanocrystals remain similar in size and morphology with an average particle size of $11.1 \pm 3.0 \text{ nm}$, after heating to 180 °C for 4 h to release the

hydrogen and re-generate Pd.

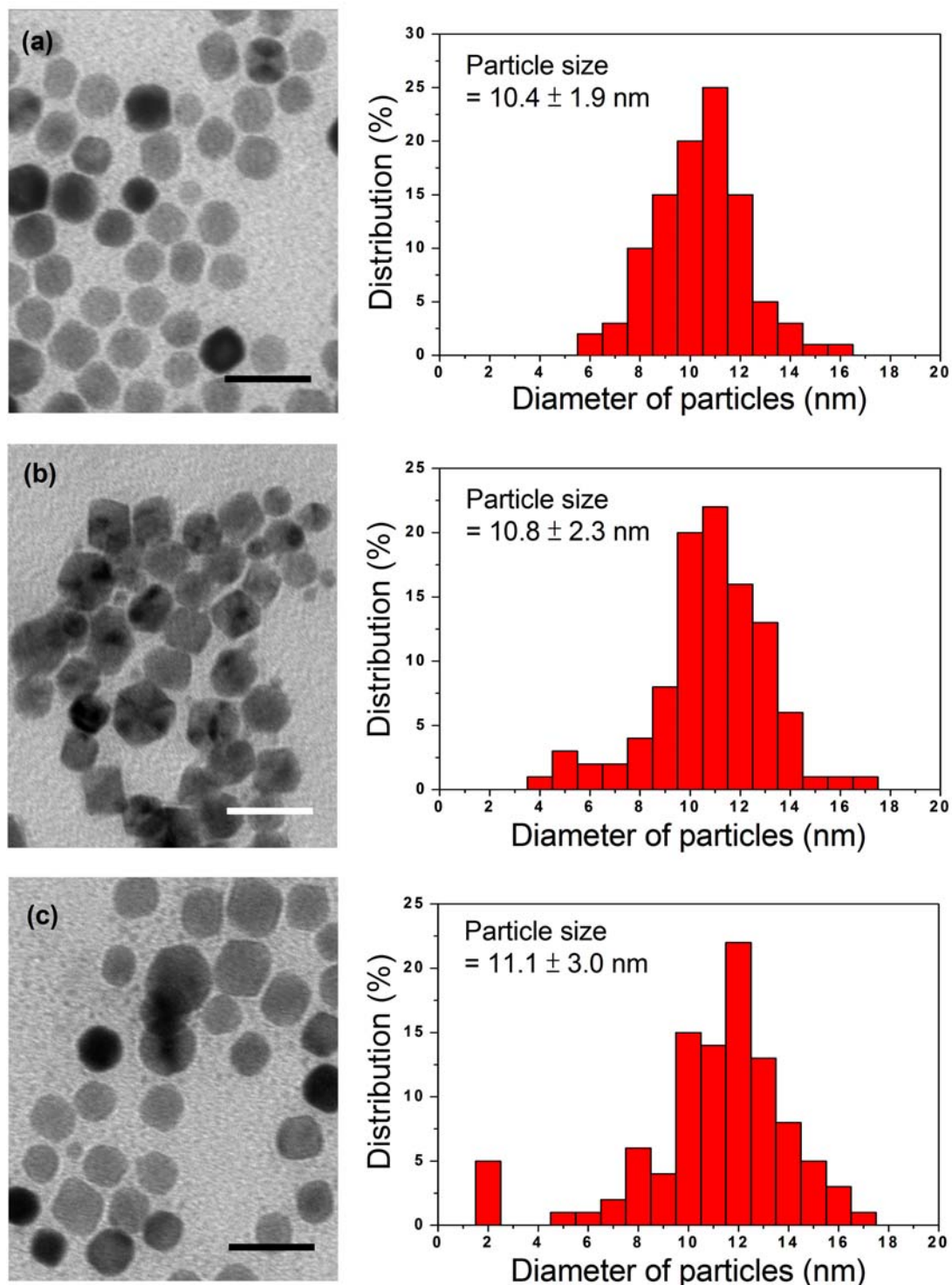


Fig 1-6 TEM images and corresponding particle size distributions of (a) Pd nanocrystals, (b) PdH_x nanocrystals after reaction with NaBH₄ in TEG, and (c) re-generated Pd nanocrystals after hydrogen release. Scale bars in (a), (b), and (c) correspond to 20 nm. Percentages are based on 200 particles for each sample.

We observed the presence of ultrasmall Pd nanoparticles (~ 2 nm) in solution after heating β -PdH_x to 180 °C for 4 h, resulting in a wider particle size distribution of re-formed Pd nanocrystal. This may be attributed to the hydrogen-induced Ostwald ripening reported by Vece's group [28]. They suggested that inserting hydrogen atoms, causing separation of nearest-neighbor metals and reduction of binding energy between Pd atoms, would increase the probability of a Pd atom detaching from the particle. However, the particle size distribution of re-formed Pd nanocrystal does not increase significantly, indicating that the hydriding and dehydriding reactions can be carried out on pre-formed Pd nanocrystals and proceed with general retention of size and morphology. It is likely that the PVP stabilizer helps to prevent significant aggregation, as was observed for other nanocrystal systems prepared using similar temperatures [29]. The thermogravimetric data for the PdH_x nanocrystal under a 100 mL min⁻¹ flow of Ar is displayed in Figure 1-7.

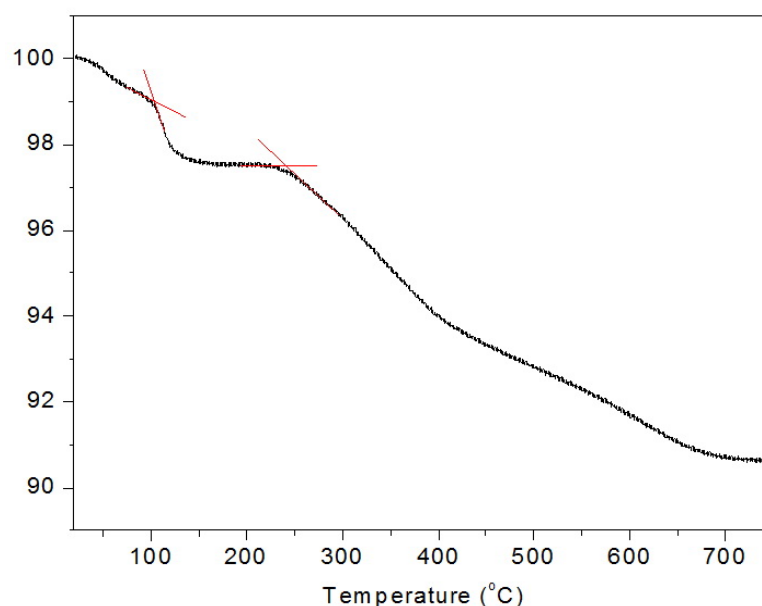


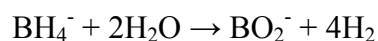
Fig 1-7 TGA data of polyol-synthesized Pd nanocrystal.

It is evident that a small decomposition step observed at 100 °C can be

attributed to the removal moisture in the sample. The second steep decomposition step obtained at 238 °C is related to the decomposition of PVP. This indicates that nanocrystalline PdH_x is stabilized effectively by PVP during dehydriding process, because the operating temperature of 180 °C in dehydriding process is lower than the decomposition temperature of PVP, 238 °C.

1.3.4 Mechanism of borohydride-assisted hydriding process

Schlesinger's group [30] reported that when reacting with H₂O, NaBH₄ rapidly undergoes hydrolysis to produce H₂ according to the following reaction equation:



The hydrogen gas decomposed from NaBH₄ may be absorbed by Pd. In order to investigate the mechanism of borohydride-assisted hydriding process, we flowed H₂ through TEG with dispersed Pd nanocrystals at 190 °C. The XRD pattern in Figure **1-8a** shows that β-PdH_x was not observed as a product upon heating Pd nanocrystals in TEG with H₂ bubbling through it, indicating that Pd would not convert into PdH_x in solution via simply absorbing H₂ gas decomposed from NaBH₄. Moreover, we attempted to convert bulk Pd into β-PdH_x by applying H₂O as solvent in a teflon lined autoclave at 190 °C for 1.5 h. Comparing with TEG, using H₂O as solvent facilitates NaBH₄ hydrolysis, producing pressurized hydrogen in an autoclave. The pressurized hydrogen has the capability of inserting into Pd lattice at 190 °C. However, the XRD pattern in Figure **1-8b** shows that only a small amount of the sample converts to β-PdH_x, based on the emergence of shoulders to the left of the *111* and *200* peaks of Pd. This result further supports the hypothesis that the H₂ is not the most important factor in the solution-based hydriding process.

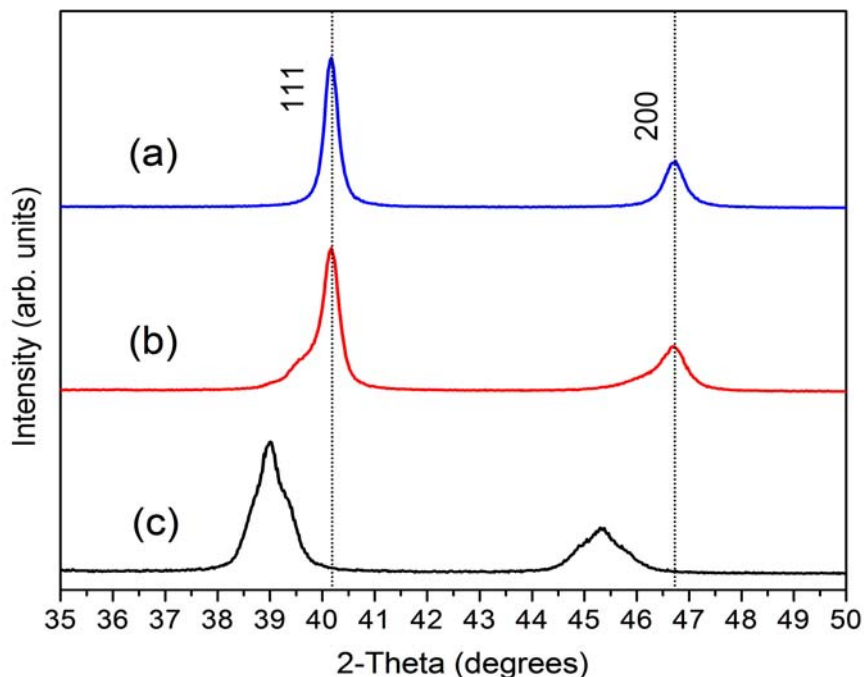
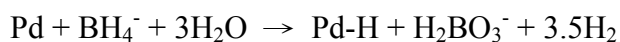


Fig 1-8 Powder XRD patterns for (a) bulk Pd reacted with bubbling H₂ in TEG at 190 °C, (b) bulk Pd reacted with NaBH₄ in H₂O in an autoclave at 190 °C, (c) bulk Pd reacted with NaBH₄ in TEG in an autoclave at 190 °C. Vertical dashed lines indicate the peak positions for Pd.

In contrast, the XRD pattern in Figure 2-8c reveals that the sample converts into β -PdH_x in an autoclave at 190 °C for 1.5 h, while using TEG as solvent. This is in agreement with the results of Murphy's group [16]. They hypothesized a metal-assisted borohydride hydrolysis reaction:



They claimed BH₄⁻ has the hydriding power of ~20 to 30 atm of H₂ for bulk powders of metals and intermetallics. We suggest that the low water content in TEG would suppress NaBH₄ hydrolysis with H₂O, as well as facilitate the metal-assisted borohydride hydrolysis reaction as shown above. This indicates that the species BH₄⁻ plays a more significant role converting Pd into β -PdH_x than H₂ in the solution-based

hydriding process. Our suggestion is also consistent with the results of Guella's group [31]. They demonstrated the mechanism of Pd-catalyzed borohydride hydrolysis using ^{11}B NMR. After being chemisorbed on the surface of Pd, BH_4^- is then dissociated into the intermediate product, Pd-BH_3^- , and Pd-H . The intermediate species Pd-BH_3^- can further react with H_2O to produce Pd-H and BH_3OH^- , as shown in Figure 1-9. The dissociated hydrogen atoms chemisorbed on the Pd surface can move to subsurface sites and rapidly diffuse through the entire bulk Pd powder, converting Pd into $\beta\text{-PdH}_x$.

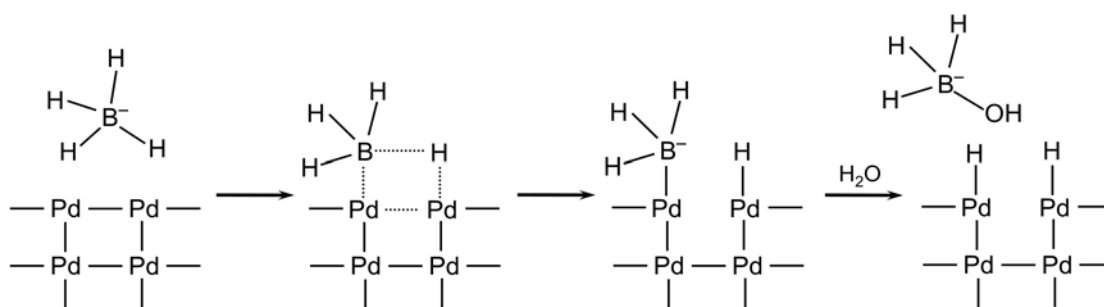


Fig 1-9 Mechanism of Pd-catalyzed borohydride hydrolysis in H_2O [31].

1.4 Conclusion

In conclusion, we have demonstrated a facile low-temperature and ambient-pressure solution-phase process for converting bulk and nanocrystalline Pd into $\beta\text{-PdH}_x$, effectively merging the polyol process for nanocrystal synthesis with metal hydride hydrogen storage materials. The experiments indicate that nanocrystalline Pd absorbs and releases hydrogen faster and at lower temperatures than bulk Pd, and results in the formation of dispersible metal hydride nanocrystals with general size and morphology retention relative to the metal nanoparticle templates. This conclusion is consistent with the previous hydrogen uptake studies for Pd nanocrystals reported by Horinouchi's group [18]. We also provided

supporting evidence for the mechanism of the solution-phase borohydride-assisted hydriding process. Pd would not convert into PdH_x via simply absorbing H₂ gas decomposed from NaBH₄, but through dissociating BH₄⁻ and then absorbing chemisorbed H atoms into its lattice.

In analogy to similar chemistry in non-hydride systems, other available shapes of Pd nanoparticles, including rods, bars, and plates [23], should provide access to analogous shapes of PdH_x nanoparticles that would be useful for studying the properties of shape-controlled metal hydride nanocrystals. This chemistry should also be portable to other metal and alloy systems, perhaps opening the door to a library of colloidal metal and intermetallic hydride nanocrystals with enhanced hydrogen absorption and release capabilities.

References

1. Alefeld, G.; Volkl, J. Eds. *Hydrogen in metals II*; Springer: Berlin Heidelberg, 1978. p. 73-155.
2. Shan, X.; Payer, J.H.; Wainright, J.S., *Increased performance of hydrogen storage by Pd-treated $\text{LaNi}_{4.7}\text{Al}_{0.3}$, CaNi_5 and Mg_2Ni* . Journal of Alloys and Compounds, 2006. **426**: p. 400-407.
3. Shan, X.; Payer, J.H.; Wainright, J.S., *Improved durability of hydrogen storage alloys*. Journal of Alloys and Compounds, 2007. **430**: p. 262-268.
4. Sabo, M.; Henschel, A.; Frode, H.; Klemm, E.; Kaskel, S., *Solution infiltration of palladium into MOF-5: synthesis, physisorption and catalytic properties*. Journal of Materials Chemistry, 2007. **17**: p. 3827-3832.
5. Jung, J.H.; Rim, J.A.; Lee, S.J.; Cho, S.J.; Kim, S.Y.; Kang, J.K.; Kim, Y.M.; Kim, Y.J., *Pd-doped double-walled silica nanotubes as hydrogen storage material at room temperature*. The Journal of Physical Chemistry C, 2007. **111**: p. 2679-2682.
6. Lin, Y.-M.; Rei, M.-H., *Separation of hydrogen from gas mixture out of catalytic reformer by using supported palladium membrane*. Separation and Purification Technology, 2001. **25**: p. 87-95.
7. Im, Y.; Lee, C.; Vasquez, R.P.; Bangar, M.A.; Myung, N.V.; Menke, E.J.; Penner, R.M.; Yun, M., *Investigation of a single Pd nanowire for use as a hydrogen sensor*. Small, 2006. **2**: p. 356-358.
8. Skoskiewicz, T., *Superconductivity in palladium-hydrogen and palladium-nickel-hydrogen systems*. Physica Status Solidi A-Applied Research, 1972. **11**: p. K123.
9. Strizker, B.; Buckel, W., *Superconductivity in palladium-hydrogen and the palladium-deuterium systems*. Zeitschrift fur Physik, 1972. **257**: p. 1-8.
10. Maeland, A.J.; Flanagan, T.B., *Lattice constants and thermodynamic parameters of the hydrogen-platinum-palladium and deuterium-platinum-palladium systems*.

The Journal of Physical Chemistry, 1964. **68**: p. 1419-1426.

11. Maeland, A.J.; Bibb, Jr. T.R.P., *X-ray diffraction observations of the Pd-H₂ system through the critical region*. The Journal of Physical Chemistry, 1961. **65**: p. 1270-1272.
12. Schirber, J.E.; Morosin, B., *Lattice constants of β -PdH_x and β -PdD_x with x near 1.0*. Physical Review B, 1975. **12**: p. 117-118.
13. Owen, E.A.; Williams, E.S.J., *X-ray study of the hysteresis effect observed in the palladium-hydrogen system*. Proceedings of the Physical Society, 1944. **56**: p.52-63.
14. Antonov, V.E.; Belash, I.T.; Malyshev, V.Y.; Ponyatovsky, E.G., *The solubility of hydrogen in the platinum metals under high pressure*. International Journal of Hydrogen Energy, 1986. **11**: p. 193-197.
15. Bernardini, M.; Comisso, N.; Fabrizio, M.; Mengoli, G.; Randi, A., *Effect of temperature on electrolytic loading of hydrogen into palladium*. Journal of Electroanalytical Chemistry, 1998. **453**: p. 221-230.
16. Murphy, D.W.; Zahurak, S.M.; Vyas, B.; Thomas, M.; Badding, M.E.; Fang, W.-C., *A new route to metal hydrides*. Chemistry of Materials, 1993. **5**: p. 767-769.
17. Balde, C.P.; Hereijgers, B.P.C.; Bitter, J.H.; de Jong, K.P.; *Sodium alanate nanoparticles – linking size to hydrogen storage properties*. Journal of the American Chemical Society, 2008. **130**: p. 6761-6765.
18. Horinouchi, S.; Yamanoi, Y. Yonezawa, T.; Mouri, T.; Nishihara, H., *Hydrogen storage properties of isocyanide-stabilized palladium nanoparticles*. Langmuir, 2006. **22**: p. 1880-1884.
19. Yamauchi, M.; Ikeda, R.; Kitagawa, H.; Takata, M. *Nanosize effects on hydrogen storage in palladium*. The Journal of Physical Chemistry C, 2008. **112**: p. 3294-3299.
20. Vasquez, Y.; Luo, Z.P.; Schaak, R.E., *Low-temperature solution synthesis of the non-Equilibrium ordered intermetallic compounds Au₃Fe, Au₃Co, and Au₃Ni as*

- nanocrystals*. Journal of the American Chemical Society, 2008. **130**: p. 11866-11867.
21. Dawood, F. and Schaak, R.E., *ZnO-templated synthesis of wurtzite-type ZnS and ZnSe nanoparticles*. Journal of the American Chemical Society, 2009. **131**: p. 424-425.
 22. Ducampsanguesa, C.; Herreraurbina, R.; Figlarz, M., *Fine palladium powders of uniform particle size and shape produced in ethylene glycol*. Solid State Ionics, 1993. **63-65**: p. 25-30.
 23. Xia, Y.N.; Xiong, Y.J.; Lim, B.K.; Skrabalak, S.E., *Shape-controlled synthesis of metal nanocrystals: simple chemistry meets complex physics?*. Angewandte Chemie - International edition, 2009. 48: p. 60-103.
 24. Xiong, Y.J.; Chen, J.Y.; Wiley, B.; Xia, Y.N., *Understanding the role of oxidative etching in the polyol synthesis of Pd nanoparticles with uniform shape and size*. Journal of the American Chemical Society, 2005. **127**: p. 7332-7333.
 25. Amorim, C.; Keane, M.A., *Palladium supported on structured and nonstructured carbon: A consideration of Pd particle size and the nature of reactive hydrogen*. Journal of Colloid and Interface Science, 2008. **322**: p. 196-208.
 26. Millet, P., *Thermodynamic paths in the two-phases domain of the PdH system and a method for kinetic analysis*. Electrochemistry Communications, 2005. **7**: p. 40-44.
 27. Kishore, S.; Nelson, J.A.; Adair, J.H.; Eklund, P.C., *Hydrogen storage in spherical and platelet palladium nanoparticles*. Journal of Alloys and Compounds, 2005. **389**: p. 234-242.
 28. Di Vece, M.; Grandjean, D.; Van Bael, M.J.; Romero, C.P.; Wang, X.; Decoster, S.; Vantomme, A.; Lievens, P., *Hydrogen-induced ostwald ripening at room temperature in a Pd nanocluster film*. Physical Review Letters, 2008. **100**: p. 236105.
 29. Sra, A.K. and Schaak, R.E., *Synthesis of atomically ordered AuCu and AuCu₃ nanocrystals from bimetallic nanoparticle precursors*. Journal of the American

Chemical Society, 2004. **126**: p. 6667-6672.

30. Schlesinger, H.I.; Brown, H.C.; Hoekstra, H.R.; Rapp, L.R., *Reactions of diborane with alkali metal hydrides and their addition compounds. New syntheses of borohydrides. Sodium and potassium borohydrides*. Journal of the American Chemical Society, 1953. **75**: p. 199-206.
31. Guella, G.; Zanchetta, C.; Patton, B.; Miotello, A., *New insights on the mechanism of palladium-catalyzed hydrolysis of sodium borohydride from ^{11}B NMR measurements*. The Journal of Physical Chemistry B, 2006. **110**: p. 17024-17033.

Appendix

Resume

Education

The Pennsylvania State University, University Park, PA Aug. 2006 - Aug. 2009
Master of Science in Chemistry (Transferred with R.E. Schaak from Texas A&M University, College Station, TX, - August 2007)

◆ GPA: 3.2/4.00

National Tsing Hua University (NTHU), Hsinchu, Taiwan Sept. 2000 - Jan. 2005
Bachelor of Science in Chemistry

◆ Junior-Senior GPA: 3.74/4.00

◆ Minor: Materials Science and Engineering

Publications

1. Phan, T.H. and Schaak, R.E., *Polyol synthesis of palladium hydride: bulk powders vs. nanocrystals*. Chemical Communications, 2009. **23**: p. 3026-3028
2. Leonard, B.M.; Anderson, M.E.; Oyler, K.D.; Phan, T.H.; Schaak, R.E., *Orthogonal reactivity of metal and multimetal nanostructures for selective, stepwise, and spatially-controlled solid-state modification*. ACS Nano, 2009. **3**: p. 940-948.
3. Bauer, J.C.; Chen, X.; Liu, Q.S.; Phan, T.H.; Schaak, R.E., *Converting nanocrystalline metals into alloys and intermetallic compounds for applications in catalysis*. Journal of Materials Chemistry, 2008. **18**: p. 275-282.
4. Liu, P.H.; Chang, Y.P.; Phan, T.H.; Chao, K.J., *The morphology and size of nanostructured Au in Au/SBA-15 affected by preparation conditions*. Materials Science and Engineering C, 2006. **26**: p. 1017-1022.
5. Chao, K.J.; Chang, Y.P.; Chen, Y.C.; Lo, A.S.; Phan, T.H., *Morphology of nanostructured platinum in mesoporous materials - Effect of solvent and intrachannel surface*. Journal of Physical Chemistry B, 2006. **110**: p. 1638-1646.

Poster

1. Phan, T.H. and Schaak, R.E., *Solution chemistry synthesis of nanocrystalline palladium hydride*. 236th ACS National Meeting, Philadelphia, PA, United States, August 17-21, 2008